

Climate change impact on regional floods in the Carpathian region

Iulii Didovets^{a,b,*}, Valentina Krysanova^b, Gerd Bürger^a, Sergiy Snizhko^c,
Vira Balabukh^d, Axel Bronstert^a

^a Institute for Earth and Environmental Sciences, University of Potsdam, Germany

^b Potsdam Institute for Climate Impact Research, Germany

^c Taras Shevchenko National University of Kyiv, Ukraine

^d Ukrainian Hydrometeorological Research Institute, Ukraine

ARTICLE INFO

Keywords:

Climate change impact
Floods
Hydrological modelling
SWIM
Tisza
Prut
Carpathians
Ukraine

ABSTRACT

Study region: Tisza and Prut catchments, originating on the slopes of the Carpathian mountains.
Study focus: The study reported here investigates (i) climate change impacts on flood risk in the region, and (ii) uncertainty related to hydrological modelling, downscaling techniques and climate projections. The climate projections used in the study were derived from five GCMs, downscaled either dynamically with RCMs or with the statistical downscaling model XDS. The resulting climate change scenarios were applied to drive the eco-hydrological model SWIM, which was calibrated and validated for the catchments in advance using observed climate and hydrological data. The changes in the 30-year flood hazards and 98 and 95 percentiles of discharge were evaluated for the far future period (2071–2100) in comparison with the reference period (1981–2010).

New hydrological insights for the region: The majority of model outputs under RCP 4.5 show a small to strong increase of the 30-year flood level in the Tisza ranging from 4.5% to 62%, and moderate increase in the Prut ranging from 11% to 22%. The impact results under RCP 8.5 are more uncertain with changes in both directions due to high uncertainties in GCM-RCM climate projections, downscaling methods and the low density of available climate stations.

1. Introduction

In recent decades, observed climate trends show an increase in temperature across Europe (IPCC, 2014). Precipitation totals show regionally varying changes and have no clear continental trend compared to temperature. Since 1960, annual precipitation has increased by up to 70 mm per decade in Northern Europe and decreased by up to 90 mm per decade in some parts of Southern Europe (EEA, 2017). River discharge shows similar trends as in precipitation, with decreases in Southern and Eastern Europe and increases in Northern Europe (Stahl et al., 2010; Wilson et al., 2010). According to the IPCC reports (IPCC, 2014; Kovats et al., 2014), there is also a high confidence in changes in temperature extremes, heat waves and heavy precipitation events in Europe (Seneviratne et al., 2014; Donat et al., 2013). Also, an increase in climate-related hazards and their intensity is noticed, but with a less clear signal and large variation among European regions (IPCC, 2007). Changes in hydrological extremes are now anticipated to be more pronounced and might be related to changing climate conditions (IPCC, 2014).

Besides such general considerations for the whole continent, it has also been shown that changes in climate and hydrological extremes are already observed in several regions, e.g. changes in rainfall totals (IPCC, 2014), rainfall intensity (e.g. Mueller and

* Corresponding author at: Potsdam Institute for Climate Impact Research (PIK), Telegraphenberg A 31, 14473 Potsdam, Germany.

E-mail address: didovets@uni-potsdam.de (I. Didovets).

<https://doi.org/10.1016/j.ejrh.2019.01.002>

Received 12 March 2018; Received in revised form 26 December 2018; Accepted 1 January 2019

Available online 16 February 2019

2214-5818/ © 2019 The Authors. Published by Elsevier B.V. This is an open access article under the CC BY-NC-ND license (<http://creativecommons.org/licenses/by-nc-nd/4.0/>).

Pfister, 2011), flooding rates (e.g. Huang et al., 2013) and timing and seasonality of flooding (e.g. Vormoor et al., 2015). Some increases in extreme river discharge have been observed for a number of gauging stations over Germany (e.g. Petrow et al., 2009), Central Europe (e.g. Villarini et al., 2011) and France (e.g. Renard et al., 2008). Also, changes in the timing of floods have been detected in river basins around the North Sea and in Eastern Europe (Blöschl et al., 2017). For alpine catchments Kormann et al. (2015) have shown that the hydrological regimes, including flood regimes, of high mountain rivers are changing slowly but steadily.

There were several ruinous floods in recent decades (in 1998, 2001 and 2008) in Ukraine (Kovalets et al., 2014). One of the biggest and destructive floods occurred in the Carpathian region and surrounding areas within Ukraine, Moldova and Romania at the end of July 2008, causing 47 fatalities and evacuation of about 40 000 people (World Health Organization, 2017). Over 40.000 houses and 33.000 ha of farmland were flooded in Ukraine (International Commission for the Protection of the Danube River (ICPDR) (2009)).

Many studies done recently have been dedicated to future changes of climate in Europe. The climate projections under different emission scenarios show a temperature increase over Europe in the range from 1 to 4.5 °C under RCP 4.5 and 2.5 to 5.5 °C under RCP 8.5 by the end of the century (EEA, 2017); with higher increases for Southern Europe in summer, and Northern and Eastern Europe in winter (Kjellström et al., 2011; Mitchell et al., 2004).

Annual precipitation totals show a less clear signal of change in the 21st century compared to temperature, although there is agreement of most projections on an overall annual increase in Northern Europe of up to 30%, and decrease in Southern Europe of up to 40% by the end of the century (Jacob et al., 2014; Kjellström et al., 2011). An increasing trend for extreme precipitation by the end of the century was also claimed for Northern Europe (IPCC, 2014), although the uncertainty of such projection is very high. However, recent studies on extreme rainfall intensities over recent decades have shown that an increasing trend of high intensity rain storms can be identified for several regions in Central Europe if one investigates short time increments, i.e. between a few minutes to one hour (see, e.g., Mueller and Pfister, 2011 and Bürger et al., 2014).

Changing climate will affect river discharge. The future changes in the mean and extreme river discharge can be regionally different. In some studies, there are indications of a shift in seasonality of river discharge and floods, with increases in winter and autumn and decreases in spring e.g. in Finland (Veijalainen et al., 2010) and Norway (Vormoor et al., 2015). Also, increases in high flow and 10-year flood level were found in France (Quintana-Seguí et al., 2011).

In contrast, the decreases in 10-year flood and mean annual flood were projected for the Alpine Lech catchment, with a significant increase in winter floods (Dobler et al., 2012). In another study for the Alps, the mean annual floods and maximum floods are projected to increase in Switzerland, and to decrease in the Southern Alps (Köplin et al., 2014). The study of Meresa et al., 2017 focused on a mountain catchment in Poland projected an increase in the annual maximal flow by the end of the century.

Increasing trends in temperature were observed in Ukraine (Balabukh and Lukianets, 2015; Kynal and Kholiavchuk, 2016; Spinoni et al., 2015). However, no changes in the observed annual maximum river discharge were found in the rainfall and snowmelt driven rivers in mountainous areas within Ukraine for the last 60 years (Gorbachova and Barandich, 2016).

Despite the large number of papers focusing on climate change impacts on extremes in Europe, there are only a few studies on changes in extreme precipitation and river discharge done for Eastern Europe (Meresá et al., 2017; Piniewski et al., 2017), and in particular for Ukraine (Didovets et al., 2017; Krakovska et al., 2012). Therefore, keeping in mind the ruinous floods in the past and expected climate change, it is necessary to conduct an assessment of current and expected trends in flood magnitude and frequency in Ukraine under warming climate, especially in the vulnerable region of the Carpathian Mountains.

Hence, the main purpose of this research is to assess the impacts of climate change on high flows and flood frequency and magnitude in the mountainous Carpathian region of Ukraine. In addition, the impacts based on the dynamical and statistical downscaling methods are compared, and uncertainties related to climate projections, downscaling techniques and hydrological modelling are discussed. The Carpathian is characterised as a data-scarce region with highly variable meteorological and hydrological conditions, and therefore it was decided to combine regional observations with globally available data for this investigation. The study was performed for two catchments in the region: the Upper Tisza and the Upper Prut.

The climate projections were derived from five General Circulation Models (GCMs) downscaled with a Regional Climate Models (RCMs) and with the statistical downscaling model XDS. Two Representative Concentration Pathways (RCP), RCP 4.5 and RCP 8.5, were applied.

The eco-hydrological SWIM model driven by the climate projections was used to simulate hydrological cycle in the basins under study with the focus on high flows and floods. The model was calibrated and validated in advance for two outlet gauges, and additionally checked for two extra gauges in the upstream parts of the studied basins. The results of simulations based on climate projections under RCP 4.5 and RCP 8.5 emission scenarios in the “far future” period (2071–2100) were compared with simulations in the reference period (1981–2010) driven by the same climate models. Finally, the uncertainty in the projected high flows and floods was analysed.

2. Study area

The Tisza and Prut rivers are tributaries of the Danube River. Their catchment areas are shared by several countries: Ukraine, Romania, Hungary, Slovakia, Serbia and Moldova. The catchments of the Upper Tisza and Upper Prut (in the following referred to as Tisza and Prut) in the Carpathian region (Fig. 1) were selected as study areas. Due to data scarcity and missing data on water management only the upper parts of the river catchments were considered. The major part of our study areas lies within Ukraine and covers approximately a half of the mountain region of Ukrainian Carpathians. This region is also important as water source for the whole Danube catchment. Both rivers are essential for the local population, as the Tisza catchment covers the whole Zakarpattia



Fig. 1. Two catchments under study in the Carpathian region, and the location of selected climate stations and discharge gauges.

Oblast (Ukraine) and the Prut catchment partly covers Ivano-Frankivsk and Chernivtsi Oblasts with total population of more than 2 million people. They are the main sources of water for domestic, agricultural and industrial use.

The drainage areas of the Tisza and Prut catchments are 9530 km² and 9300 km², respectively. The climate in both catchments is temperate, with average annual precipitation of 1100 mm in the Tisza catchment and 758 mm in the Prut catchment. In the period from 1980 to 2000, the mean monthly temperatures in January/July were -3.9/ + 16.9 °C in the Tisza, and + 3.9 °C / + 17.5 °C in the Prut catchment. The average discharge at the Vilok gauge in the Tisza is 206 m³/s (1992–2010), and it is 80 m³/s at the Radauti gauge in the Prut (1980–2000).

The hydrological regimes of both catchments are snowmelt and rainfall-driven. The minimum runoff is observed in the fall–winter period for the Prut catchment, and in the summer–fall period for the Tisza catchment. The basins have different flood regimes and timing: in recent years the majority of floods occurred in November–December and spring months in the Tisza, and in the late spring and summer months in the Prut (Fig. 2). This can be explained by differences in the catchments' shapes, climate conditions, topography and land use.

The average annual precipitation is higher in the Tisza compared to the Prut catchment. This can be explained by prevailing of western air masses coming to the region, and the windward and leeward side conditions that take place in the catchments. The western air masses bring wet conditions firstly to the Tisza catchment, and after that, partly retained by mountains, to the Prut catchment. Also, the percentage of area covered by mountains in the Tisza catchment is much higher. The altitudes of both catchments range between 90–95 m a.s.l. at the outlets and 2100 m a.s.l. in the headwaters. However, the percentage of area with an elevation above 600 m a.s.l. is over 70% in the Tisza catchment, and only 34% in the Prut catchment. The Tisza catchment stretches from north-west to the south-east along the Carpathian Mountains. It allows to accumulate more water from precipitation compared to the Prut, which stretches from west to east.

Also, the prevailing land use types in the catchment (forest in the Tisza and crops in the Prut) play important roles in defining their hydrological regimes and flood timing. In the mountainous areas forest can delay hydrological responses of river runoff after intense precipitation events and slow down snowmelt process in case of a rapid increase of air temperature in spring. But in the case of deforestation there could be opposite effects and an additional risk of erosion.

Most floods that occur in fall–winter seasons in the Tisza river are generated by a combination of rapid increase in the air temperature, causing snow melt, and heavy precipitation events. In the Prut catchment, such conditions are also possible, but there is no such a pronounced overarching response of snowmelt and rainfall generated floods due to lower elevation and more narrow and long shape of the catchment.

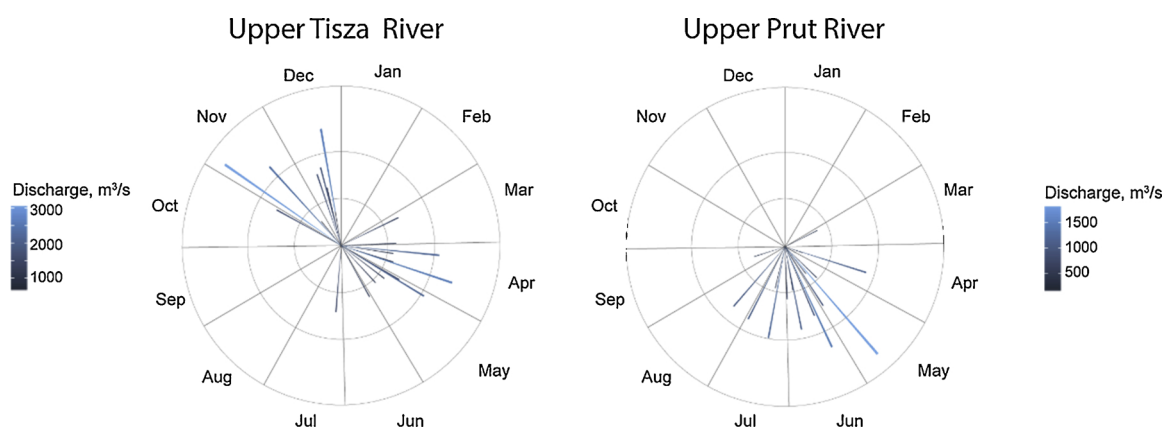


Fig. 2. Seasonality of current flood regimes in the catchments under study displayed by flood roses, indicating the magnitude and timing of the observed annual maximum floods in the period from 1980 to 2000.

The main land cover classes in the Tisza catchment are forest (deciduous, evergreen and mixed, 56.2%) and cropland (8.5%). The Prut catchment has a different structure: the main land cover classes are cropland (47%), evergreen forest (22%) and grassland (8.8%). Both rivers are regulated by dams and ponds. There are nine reservoirs, with a total volume of 60.5 hm³ in the Ukrainian part of the Tisza catchment, and they are mostly used for seasonal water regulation, fishing and amelioration purposes. There are no big reservoirs in the Prut catchment, but many ponds in the downstream part. It was not possible to include water management in the modelling due to the lack of adequate management data for these catchments.

3. Data and methods

3.1. SWIM

The eco-hydrological model SWIM is a process-based semi-distributed model. SWIM is based on two previously developed models: MATSALU (Krysanova et al., 1989) and SWAT (Arnold et al., 1993), and implements the hydrological cycle, nutrients cycles (nitrogen and phosphorus), vegetation growth and sediment transport at the river basin scale.

The model was developed mainly for impact studies in mesoscale and large river basins. SWIM has a three-level disaggregation scheme: basin – sub-basins – hydrotopes. Hydrotopes are homogeneous spatial sets of units within sub-basins obtained by overlapping land use, soil and sub-basin map layers. The climate data are interpolated to centroids of sub-basins, and are considered homogeneous at the sub-basin level. The inverse distance method was implemented for the climate data interpolation. The model SWIM considers the climate data on the sub-basin level homogeneously, but precipitation and temperature were corrected at the hydrotope level during calibration of the model based on simple elevation dependencies and applied for all period of modelling.

The model was intensively tested and has been applied for impact assessments in more than 50 catchments worldwide, particularly in Europe (Hattermann et al., 2008; Huang et al., 2013), Asia (Krysanova et al., 2015), America (Huang et al., 2016; Koch et al., 2015), and Africa (Aich et al., 2014). The model continues to be developed further, e.g. glacier and reservoir modules were recently included and tested (Koch et al., 2013; Lobanova et al., 2017; Wortmann et al., 2016).

To assess the model performance for simulation of river discharge, the Nash-Sutcliffe efficiency (NSE) (Nash and Sutcliffe, 1970) and percent bias (PBIAS) (Gupta et al., 1999) criteria were used in the study. Also the annual maxima and return levels of floods were compared for the Tisza and Prut river catchments.

The SWIM model was calibrated and validated for the Tisza and Prut river catchments for the period from 1980 to 2000. In both cases, the first half of the period was taken for calibration, and second for validation. The observed river discharge from the Vilok and Tiszabecs gauges in the Tisza and from the Radauti and Chernivtsi gauges in the Prut was used. Data for the Vilok and Tiszabecs gauges were available only for a part of the whole period: from 1990 to 2000 and from 1980 to 1992, correspondingly. Therefore, it was decided to combine data and to calibrate the model for the Tiszabecs, and validate it for the Vilok gauge, because the gauges are located very close to each other on the Hungary–Ukraine border. For the Prut catchment, the model was calibrated and validated for the Radauti gauge, and additionally verified for the Chernivtsi gauge.

Since both catchments are located in the mountains, they are snowmelt and rainfall driven. The sensitivity analysis was performed in advance for the curve number parameters of soils, groundwater and evapotranspiration related parameters. The most sensitive parameters during the calibration were related to snowmelt, runoff generation and routing processes.

3.2. Input data

For the SWIM model setup the following data are needed: land use, digital elevation model (DEM), soil map with the soil profile parametrisation, and climate data (daily minimal, maximal and average temperature, precipitation, solar radiation, air humidity and

solar radiation).

For this study, a DEM was obtained from the Shuttle Radar Topography Mission (SRTM) of the CGIAR Consortium for Spatial Information. The spatial resolution of the DEM is 90 m with appropriate correction (CGIAR-CSL, 2017).

Due to the absence of land use maps in digital form, the data was derived from different open sources (Open Street Map contributors, 2017; Patterson and Kelso, 2016; U.S. Dept. of the Interior, 2005) and also by classification of satellite images (U.S. Geological Survey, 2016). The 30 m resolution map derived for the catchments under study was reclassified to the SWIM required format (15 classes: water, settlement, industry, road, bare soil, cropland, meadow, pasture, set-aside, evergreen forest, deciduous forest, mixed forest, wetland, heather, and glaciers).

The soil map and a partial parametrization of soil layers were obtained from the Harmonized World Soil Database created by the Food and Agriculture Organization of the United Nations with 1 km resolution (FAO/IIASA/ISRIC/ISSCAS/JRC, 2012). The data were prepared and converted to the SWIM format, and some missing parameters such as porosity, field capacity, saturated conductivity and erodibility factor were estimated with pedotransfer functions (Wosten et al., 2001).

Some of the necessary climate data (daily minimal, maximal and average temperatures and precipitation) were obtained for the period 1980–2000 from 12 climate stations located in the area under study (Fig. 1). The majority of stations are located in lowland, and only one station is located at elevation above 900 m a.s.l. The average climate station density is 1 station per 2500 km². Other necessary climate variables (air humidity, solar radiation, wind) were not available. Therefore it was decided to add these variables from the reanalysis data “WATCH Forcing Data ERA-Interim” (WFDEI) (Weedon et al., 2014), and to combine them with the observed ones.

Also, precipitation data obtained from WFDEI and Global Precipitation Climatology Centre (GPCC) were considered as potential inputs to the SWIM model. But GPCC and WFDEI data showed underestimation during the whole year in comparison to the observed data. Due to that and low spatial resolution (in case of GPCC – $1 \times 1^\circ$) it was decided to use the observed precipitation data. The discharge data were obtained from the Global Runoff Data Centre (GRDC, 56068 Koblenz) for three runoff gauges, and from the Ukrainian Hydrometeorological Center for one gauge. The Prut River dynamics are represented by the daily discharge from the Radauti gauge located in Romania for the period from 1960 to 2008. River discharge for the Tisza catchment was obtained for the Tiszabecs gauge in Hungary for the period 1937–1995 and the Vilok gauge in Ukraine for the period 1992–2010. The Tiscabecs and Vilok gauges are located close to each other on the Ukrainian-Hungary border, and have very similar hydrographs.

3.3. Climate scenarios

3.3.1. Climate scenarios downscaled by RCMs from the European IMPRESSIONS project

A set of seven climate scenarios provided by the European IMPRESSIONS project (“Impacts and Risk from High-End Scenarios: Strategies for Innovative Solutions”, www.impressions-project.eu) was used in this study. The scenarios are based on five General Circulation Models that have been dynamically downscaled using the Regional Climate Models and bias corrected to the reanalysis data WFDEI (Kok et al., 2015a) (Fig. 3, upper part). The climate projections are represented by the GCM-RCM climate simulations under RCP 4.5 and RCP 8.5 pathways with resolutions of 0.5° . The climate scenarios were selected to cover the magnitude of temperature change for period 2071–2100 compared to 1981–2010 in the range from 1 to 1.4 to above 4° (Kok et al., 2015), and include not all combinations of GCMs and RCPs. The applied climate scenarios for RCP 4.5 are: GFDL-ESM2M/RCA4, HadGEM2-ES/RCA4 and MPI-ESM-LR/CCLM4; and for RCP8.5: GFDL-ESM2M/RCA4, HadGEM2-ES/RCA4, CanESM2/CanRCM4 and IPSL-CM5A-MR/WRF.

For the bias correction, the empirical quantile method was used (Kok et al., 2015b). The period from 1981 to 2010 was taken as the basis for the correction. Each climate variable (precipitation, mean, maximum and minimum temperatures, solar radiation and specific humidity) was corrected independently, one by one (Thiemeßl et al., 2012). For this study, two emission scenarios were chosen, RCP4.5 and RCP 8.5, and all seven climate scenarios were applied (denoted as: GCM-R-45 or GCM-R-85, see Fig. 3, in the following referred to as GCM-RCM scenarios).

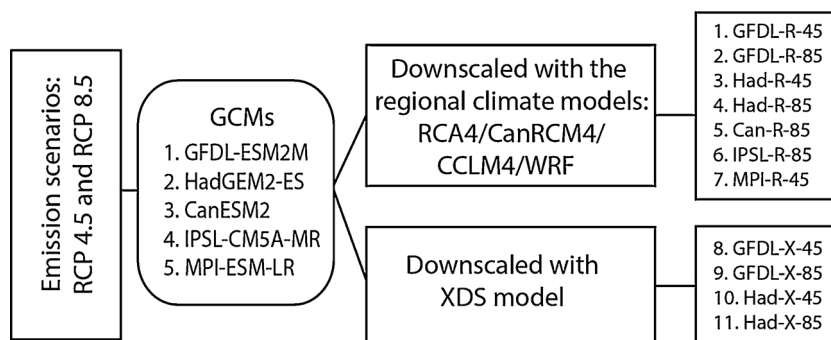


Fig. 3. The structure of climate projections based on five GCMs downscaled with RCM and with the XDS model under the RCP 4.5 and RCP 8.5 emission scenarios.

3.3.2. Four scenarios downscaled by the statistical-empirical method

The Expanded downscaling method (XDS) (Bürger, 1996) is a statistical-empirical technique for downscaling which extends the method of multiple linear regression (MLR) in a way aimed in generating more realistic multivariate local statistics. The idea is to reproduce the local meteorology as close as possible to the simulated general atmospheric circulation but at the same time taking into account the local co-variability aspects. Like MLR, the method determines a multivariate linear function between the large scale variables and the local data. The preservation of local covariance is conditioned on the (observed or simulated) global covariance, so that when driven by global data whose statistics may be altered, e.g. by climate change, the local covariability would change accordingly. This aspect of preservation and alteration of local covariances makes the technique particularly suited for the simulation of extreme events.

We used the ERA interim reanalysis data (WFDEI) and local data from climate stations for the XDS calibration. After that, XDS was applied to the GFDL-ESM2M and HadGEM2 projections under the RCP4.5 and RCP8.5 pathways (Fig. 3, lower part) to produce the following atmospheric variables: minimum, maximum and average daily temperatures, specific humidity at the 850 hPa level and surface precipitation. The period 1981–1990 was selected for calibration, and period 1991–1999 for validation. Local observations were taken from 12 local climate stations and from the WFDEI data for the considered catchments.

The XDS technique produced good results when driven by reanalysis and the GCM simulations (in the following referred to as GCM-XDS) for the period 1981–1999, based on the comparison of downscaled daily average, maximum, and minimum temperatures and precipitation for 12 climate stations with actual observations. The correlation of the modelled variables with the measurements for the calibration and validation periods is presented in Table 1. The correlation was calculated for all 12 climate stations for two periods: calibration and validation by using daily data and averaged over 12 stations. The high correlation obtained for precipitation in the mountainous area is quite surprising.

3.4. Extreme value analysis of flood level

To analyse climate induced changes in flood level, the Generalised Extreme Value distribution (GEV) (see more details in Coles, 2001) was applied in this study. The GEV distribution was used to fit the annual maximum discharges, and estimate changes in the 30-year flood levels. The GEV distribution incorporates three probability distributions (Gumbel, Frechet and Weibull), and has three parameters: location parameter, scale parameter and shape parameter. We employ a block-maximum approach, which means that for each year we pick the maximum flow event, and neglect all other high flow events. The GEV distribution function is commonly used for climate impact assessment on floods, and was applied in other studies (e.g. Dankers et al., 2007; Huang et al., 2013).

In addition, the means and 98 and 95 percentile values were estimated for the reference (1980–2010) and far future (2070–2100) periods and compared to evaluate future changes in river discharge.

4. Results

4.1. Model calibration and validation

The obtained results of calibration are between “good” and “very good” (according to thresholds proposed by Moriasi et al. (2007)). The NSE for the Tisza (Tiszabecs gauge) is 0.69 and PBIAS -15.2% in the calibration period, and 0.78 and -11.3% (Vilok gauge) in the validation period, correspondingly. The results of model calibration and validation for the Prut (Radauti gauge) are: NSE = 0.81, PBIAS = 0.2% for the calibration, and NSE = 0.67, PBIAS = 6.8% for the validation period.

Fig. 4 shows the GEV plots of the annual maxima for the simulated and observed discharge in the control period from 1980 to 2000 for the Tisza and Prut River catchments. As one can see, the agreement is quite good in both cases.

4.2. Analysis of climate model outputs in the historical and far future periods

The uncertainty, which is inherent in coupled climate simulations, contributes strongly to the uncertainty in simulated river discharge. The climate models uncertainty can be clearly shown by the differences between the simulated and observed climate variables in the historical period.

Table 2 presents these differences for the means and 95 and 98 percentiles of annual precipitation, average, maximum and minimum annual temperatures estimated for the Pozhezhevskia climate station located in mountains. For both downscaling schemes, RCMs and XDS, differences vary from small to large, and they are (naturally) smaller for the means than for the extremes. For precipitation, T_{\max} and T_{ave} the bias in 98 and 95 percentiles is smaller for climate simulations downscaled by XDS than by RCM. The

Table 1

Correlations of XDS-downscaled reanalyses to observed data, based on the mean over 12 climate stations, for the calibration and validation periods. (Tavr, T_{max}, T_{min} – average, maximum and minimum temperatures).

| Period | Tavr | T _{max} | T _{min} | Precipitation |
|-------------|------|------------------|------------------|---------------|
| Calibration | 0.97 | 0.95 | 0.94 | 0.82 |
| Validation | 0.96 | 0.94 | 0.93 | 0.81 |

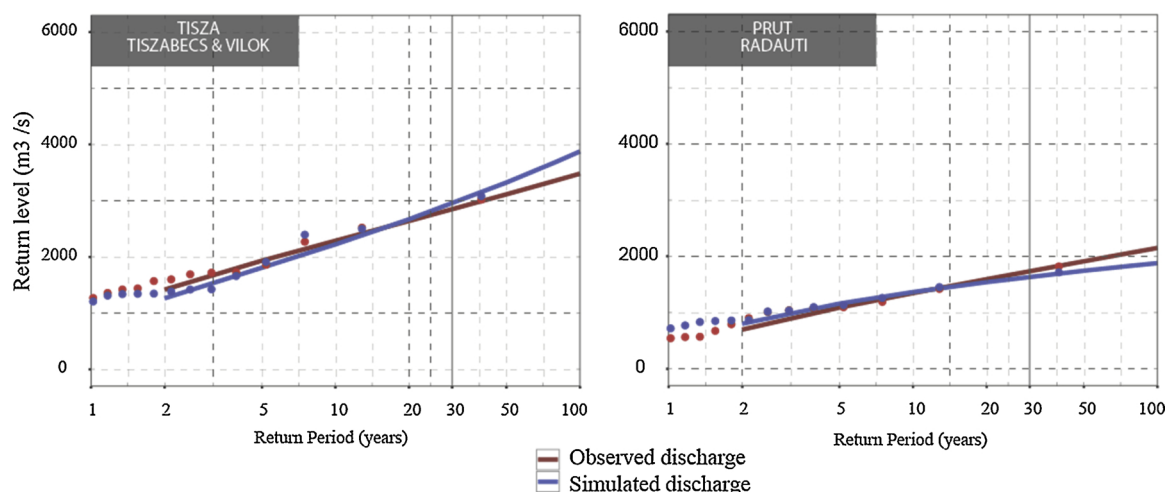


Fig. 4. Return level plots of the observed and simulated discharge levels based on the GEV distribution fit to the annual maxima discharges.

simulations downscaled by XDS have generally lower differences (except for mean P and T_{min}).

The larger differences between climate simulations downscaled by RCMs and observations, despite bias correction of the projections to the WFDEI, can be explained by poor data availability in mountainous areas (e.g. low gauge density, stations are mostly located in valleys) (Weedon et al., 2014). The lower differences produced by model runs downscaled by XDS can be explained by different approach used for downscaling. This technique calculates climate variables for the points, i.e for the locations of observation stations, and in the case of simulations downscaled by RCMs it is done for grid cells. Also, the XDS approach uses the observed climate data for historical period, and thus better performance in this period is evident. The bias of simulated climate variables for the lowland stations is lower but still moderate. The analysis for the lowland stations was done, but results are not shown in the paper.

As the next step, we analysed climate projections in the far future (2071–2100), and compared them with simulations of the same models in the reference period (1981–2010) for three representative stations: Chernivtsi and Hust in lowland and Pozhezhevskva in mountains. Table 3 summarises the results of comparison. Shown are the differences in simulated temperature and precipitation characteristics: the long-term means and the 98 and 95 percentiles, obtained from the GCM-RCM and GCM-XDS model combinations under RCP 4.5 and RCP 8.5 emission pathways.

The mean temperature shows increases in all projections for both emission pathways ranging from 0.8 °C to 6.2 °C. The HadGEM2 downscaled with XDS model projections show higher increases in mean temperature compared to other projections. Changes also depend on the emission pathway: the temperature increases under RCP 8.5 are higher compared to RCP 4.5. The higher changes in annual temperature under RCP 8.5 were expected. These GCM-RCM models were chosen in the IMPRESSIONS project to represent the “high-end” scenarios with changes of annual temperature from 1 to 1.5 to more than 4 ° in the period 2071–2100 compared to 1981–2010 (Kok et al., 2015). The similar changes in annual temperature were found for the GCM-RCM scenarios under RCP 8.5 for other catchments in Ukraine (Didovets et al., 2017).

Regarding seasonal changes in temperature, the median projections show warming during the whole year under both RCPs. The increase in fall/winter is more significant than in spring/summer, but the former one has also wider ranges of models spread.

The majority of projections show an increase in mean, 95 and 98 percentiles precipitation for the highland area (station Pozhezhevskva), but there is no clear trend for the lowland stations. In all three stations changes in mean, 95 and 98 percentiles precipitation simulated by Had-R-45, Had-R-85, Can-R-85 and IPSL-R-85 are positive, and for the last one greater than 20%. Two projections under RCP 4.5 (Had-X and Had-R) and three projections under RCP 8.5 (GFDL-X, Had-X, IPSL-R)

Table 2

Differences between the simulated and observed climate variables in the historical period (1981–2010), considering the means and 95 and 98 percentiles of precipitation, average, maximum and minimum temperatures for the Pozhezhevskva climate station.

| Scenarios | Precipitation, % | | | T max, °C | | | T ave, °C | | | T min, °C | | |
|-----------|------------------|-------|-------|-----------|------|------|-----------|------|------|-----------|------|------|
| | 0.98 | 0.95 | mean | 0.98 | 0.95 | mean | 0.98 | 0.95 | mean | 0.99 | 0.98 | mean |
| GFDL-X | -25.7 | -20.9 | -15.3 | -0.2 | 0.0 | 0.1 | 0.0 | 0.0 | 0.2 | -0.4 | 0.0 | 0.1 |
| Had-X | -21.5 | -17.4 | -13.3 | -0.8 | -0.5 | 0.0 | -0.5 | -0.3 | 0.1 | -0.5 | -0.3 | 0.0 |
| GFDL-R | -31.0 | -29.1 | -17.3 | 5.1 | 5.0 | 4.3 | 2.1 | 2.5 | 2.3 | -0.3 | -0.1 | 0.0 |
| Had-R | -29.5 | -29.7 | -16.2 | 5.2 | 5.2 | 4.3 | 2.1 | 2.4 | 2.4 | -0.9 | -0.4 | 0.1 |
| Can-R | -33.0 | -31.4 | -19.3 | 4.9 | 5.2 | 4.4 | 2.3 | 2.6 | 2.4 | -0.8 | -0.3 | 0.0 |
| IPSL-R | -32.6 | -31.4 | -17.3 | 4.2 | 4.3 | 4.3 | 2.2 | 2.5 | 2.4 | 0.0 | 0.0 | 0.0 |
| MPI-R | -34.1 | -30.9 | -16.7 | 5.4 | 5.3 | 4.5 | 2.4 | 2.7 | 2.6 | -0.7 | -0.5 | 0.3 |

Table 3

Changes in the means and 95 and 98 percentiles of the daily temperature and precipitation simulated by climate models and downscaled with RCMs and XDS for RCPs 4.5 and 8.5 in the far future (2071–2100) compared to the reference period (1980–2010) for three gauges: Chernivtsi, Hust and Pozhezhevka. Changes in precipitation indices exceeding 10% are marked by bold (positive) and underlined italic (negative) values.

| RCPs | Projections | Chernivtsi | | | | Hust | | | | Pozhezhevka | | | |
|---------|-------------|----------------------|------------------|-------------|-------------|----------------------|------------------|--------------|-------------|----------------------|------------------|-------------|-------------|
| | | $\Delta T, ^\circ C$ | Precipitation, % | | | $\Delta T, ^\circ C$ | Precipitation, % | | | $\Delta T, ^\circ C$ | Precipitation, % | | |
| | | | Avr | 0.95 | 0.98 | | Avr | 0.95 | 0.98 | | Avr | 0.95 | 0.98 |
| RCP 4.5 | GFDL-X-4.5 | 1.2 | -2.2 | -2.6 | -2.6 | 0.8 | -6.4 | -6.2 | 4.2 | 1.6 | 4.5 | 3 | 0.1 |
| | Had-X-4.5 | 3.3 | 6.2 | 7.5 | 12.5 | 3.3 | <i>-13.2</i> | -6.6 | -4.7 | 3.7 | 29.5 | 23.9 | 22.4 |
| | GFDL-R-4.5 | 1.9 | -0.5 | 0 | 4.6 | 1.6 | -1 | 2.4 | 1.1 | 1.7 | -1.6 | -2.5 | -1.7 |
| | Had-R-4.5 | 2.2 | 21.6 | 25.9 | 20.9 | 2.4 | 15.9 | 21.6 | 16.1 | 2.4 | 13.8 | 18.6 | 15.6 |
| | MPI-R-4.5 | 1.2 | -5.4 | 2.4 | 2.3 | 1.3 | -2.9 | 2 | 2 | 1.2 | -3.6 | 0 | 4.1 |
| RCP 8.5 | GFDL-X-8.5 | 2.8 | -8.4 | -6.3 | -3.3 | 2.3 | <i>-14.2</i> | -6.2 | 0 | 3.2 | 10.7 | 10.3 | 10.6 |
| | Had-X-8.5 | 5.8 | -8.2 | -3.8 | -1.5 | 5.2 | <i>-28.7</i> | <i>-16.4</i> | -7.8 | 6.2 | 57.8 | 48.3 | 51.1 |
| | GFDL-R-8.5 | 3.6 | -0.2 | 3.4 | 16.6 | 3.2 | 6.3 | 14.9 | 12.1 | 3.3 | -1.2 | 3.3 | 5 |
| | Had-R-8.5 | 4.3 | 7.4 | 11.6 | 11.9 | 4.5 | 7.1 | 14.6 | 15.5 | 4.4 | 0.2 | 8.5 | 7.4 |
| | Can-R-8.5 | 4.7 | 13.1 | 7.7 | 12.7 | 4.5 | 8.5 | 6.7 | 17.1 | 4.3 | 6.6 | 7.5 | 8.9 |
| | IPSL-R-8.5 | 4 | 29.5 | 35.6 | 50 | 3.7 | 30 | 42.4 | 43.8 | 3.8 | 20 | 30 | 26.9 |

show significant increases in all three variables in mountains exceeding 10–20% (for Had-X: 48%). Three projections under RCP 4.5 (GFDL and MPI) show small changes not exceeding 6.5% for three variables in all stations. Regarding changes in seasonality, mean precipitation under both RCPs scenarios increases during almost all months, except August and September under RCP 8.5.

Changes in the mean precipitation over sub-basins of the Prut and Tisza catchments are presented on maps in Annex 1, Figure A1 and A2. The IPSL-R-85 shows the greatest increase among all scenarios: 25–26% in both catchments. Also, the HadGEM2 projections show increases by 10–18% under RCP 4.5 in both catchments and by 12% under RCP 8.5 in the Tisza (one projection of two); this is in agreement with change signals for two stations presented in Table 3 (except Hust). And the Can-R.85 projects 10% increase in precipitation for the Prut. All other projections indicate small average changes in precipitation over the catchments not exceeding 5%.

4.3. Simulated changes in high flows and floods

Table 4 presents changes in the means, and 95 and 98 percentiles of the simulated discharge for the Tisza and Prut River

Table 4

The percentage changes in the means and 98 and 95 percentiles of simulated discharge under RCP 4.5 and RCP 8.5 emission scenarios in the far future period compared to the reference period for the Tisza and Prut River catchments (light grey colour: significant decrease ($\leq -10\%$); dark grey colour – significant increase ($\geq 10\%$)).

| RCPs | Projections | Tisza | | | Prut | | |
|------------|-------------|-------|------|------|------|------|------|
| | | 0.98 | 0.95 | mean | 0.98 | 0.95 | mean |
| RCP 4.5 | GFDL-X-4.5 | -11 | -13 | -5 | -2 | -2 | -1 |
| | Had-X-4.5 | 6 | 0 | 9 | 2 | 3 | 9 |
| | GFDL-R-4.5 | -9 | -5 | -7 | -1 | -6 | -10 |
| | Had-R-4.5 | 8 | 8 | 21 | 34 | 37 | 42 |
| | MPI-R-4.5 | 7 | -1 | -7 | -15 | -16 | -9 |
| RCP 8.5 | GFDL-X-8.5 | -25 | -23 | -17 | -19 | -24 | -21 |
| | Had-X-8.5 | -1 | -2 | -6 | -20 | -21 | -16 |
| | GFDL-R-8.5 | -14 | -10 | -6 | -1 | -9 | -13 |
| | Had-R-8.5 | -7 | -10 | -8 | 7 | 6 | -1 |
| | Can-R-8.5 | 6 | 2 | -7 | 5 | 12 | 9 |
| IPSL-R-8.5 | 11 | 12 | 41 | 66 | 56 | 60 | |

Table 5

Changes in the 30 year flood levels based on the GEV distribution fit to the annual maxima in the reference and far future periods for the Tisza and Prut catchments (Ref – reference period, FF – far future period, Dev – percent deviation).

| RCPs | Projections | Tisza | | | Prut | | |
|---------|-------------|-----------|----------|--------|-----------|----------|--------|
| | | Ref, m3/s | FF, m3/s | Dev, % | Ref, m3/s | FF, m3/s | Dev, % |
| RCP 4.5 | GFDL-X-4.5 | 1902 | 2090 | 9.9 | 747 | 879 | 17.7 |
| | Had-X-4.5 | 1882 | 1966 | 4.5 | 887 | 1084 | 22.2 |
| | GFDL-R-4.5 | 1826 | 1975 | 8.2 | 1238 | 1125 | -9.1 |
| | Had-R-4.5 | 2024 | 3272 | 61.7 | 1399 | 1552 | 10.9 |
| | MPI-R-4.5 | 2090 | 1927 | -7.8 | 879 | 994 | 13.1 |
| RCP 8.5 | GFDL-X-8.5 | 2002 | 1567 | -21.7 | 729 | 674 | -7.5 |
| | Had-X-8.5 | 1904 | 1746 | -8.3 | 881 | 690 | -21.7 |
| | GFDL-R-8.5 | 1810 | 1797 | -0.7 | 1216 | 1183 | -2.7 |
| | Had-R-8.5 | 1895 | 2664 | 40.6 | 1304 | 1831 | 40.4 |
| | Can-R-8.5 | 1820 | 1949 | 7.1 | 1200 | 1365 | 13.8 |
| | IPSL-R-8.5 | 1603 | 3199 | 99.6 | 956 | 1842 | 92.7 |

catchments driven by GCM-RCM and GCM-XDS climate projections under RCP 4.5 and RCP 8.5 emission scenarios for the far future period compared to the reference period.

Projections largely disagree on the direction and magnitude of changes in all variables for both catchments. The largest positive changes for all variables were simulated under Had-R-45 and IPSL-R-85 projections for both basins, and this agrees well with precipitation trends in [Table 3](#) and on maps in Annex 1, Figure A1 and A2. The largest negative changes are simulated for all three variables under GFDL-X-85 for both catchments and under Had-X-85 for the Prut catchment. All GFDL-based projections show negative trends under both RCPs for both catchments, ranging from -1 to -25%. Both HadGEM2-based projections show small to large positive changes under RCP45, and mostly negative changes under RCP85 (except under Had-R-85 for the Prut catchment).

Based on the simulated discharge time series in both catchments, flood frequency analyses were performed for all eleven scenario combinations. The results are shown in [Table 5](#) for the 30 year floods and in [Figs. 5 and 6](#) for flood return periods up to 100 years. However, due to the pronounced uncertainty resulting from climate scenarios and downscaling techniques, as well as limited durations of the observed discharge time series for estimation of flood levels in the reference period, it was decided to constrain the comparison of different scenario results to the 30-year flood level only.

The simulated changes in the 30-year flood for the Tisza River show a small to strong increase ranging from 4.5% to 61.7% for four projections under RCP 4.5, except one decrease by 7.8% under MPI-R-45. However, the signals of change show larger disagreement for projections under RCP 8.5: two projections indicate a decrease up to 22%, three – an increase up to 99.6% (under IPSL-R-85), and one – negligible change. The simulated changes in the 30-year flood for the Prut River are similar. Three projections show a moderate increase ranging from 11% to 22% under RCP 4.5, and one a decrease by 9% under GFDL-R-45. The changes in the Prut catchment under RCP 8.5 are also similar to those in the Tisza. Two projections show a decrease up to 22% (Had-X-8.5), three indicate an increase up to 93%, and one – small changes. In both catchments the largest change is driven by IPSL-R-8.5, and this agrees well with precipitation changes in [Table 5](#) and Annex 1, Figs. A1 and A2.

Comparing projected changes in the 30-year flood based on the XDS and RCM approaches it is clearly visible that simulations based on RCM scenarios show larger mean positive changes for the Tisza (both RCPs) and Prut (RCP 8.5) and generally larger ranges of uncertainty than simulations based on XDS in both catchments ([Fig. 5,6](#)). The model runs based on the XDS downscaling produce much smaller signals of change, which are positive for RCP 4.5 and negative for RCP 8.5 for both catchments. The difference in spreads could be partly explained by the different numbers of scenarios in two groups. This is also in agreement with the model spreads presented in [Tables 4 and 5](#) by comparing the same GCMs (Had and GFDL) for both catchments.

5. Discussion

Mountains belong to the most sensitive regions to climate change, and it is very important to study climate change impacts there, because mountain ecosystems are sources of major rivers, biodiversity and providers of vital resources to population ([Kohler et al., 2010](#)).

The climate impact assessments with the focus on floods in Europe, in particular for mountain regions, were presented by [Köplin et al. \(2014\)](#); [Roudier et al. \(2016\)](#) and [Meresa et al. \(2017\)](#) using different methods and climate projections. The results obtained in the study of [Roudier et al. \(2016\)](#) for Europe could be analysed together with our results for the Carpathian region, though a direct comparison is hardly possible due to differences in settings and methods. Anyway, some projections in both studies show similar tendencies.

The procedure for assessment of climate change impacts on hydrological extremes is usually the following: GCMs are run for different greenhouse gas emission scenarios, downscaling techniques are used to downscale GCM outputs to a region, a hydrological model is run with different downscaled climate scenarios, and statistical tools are used for the extreme value analysis ([Meresa et al.,](#)

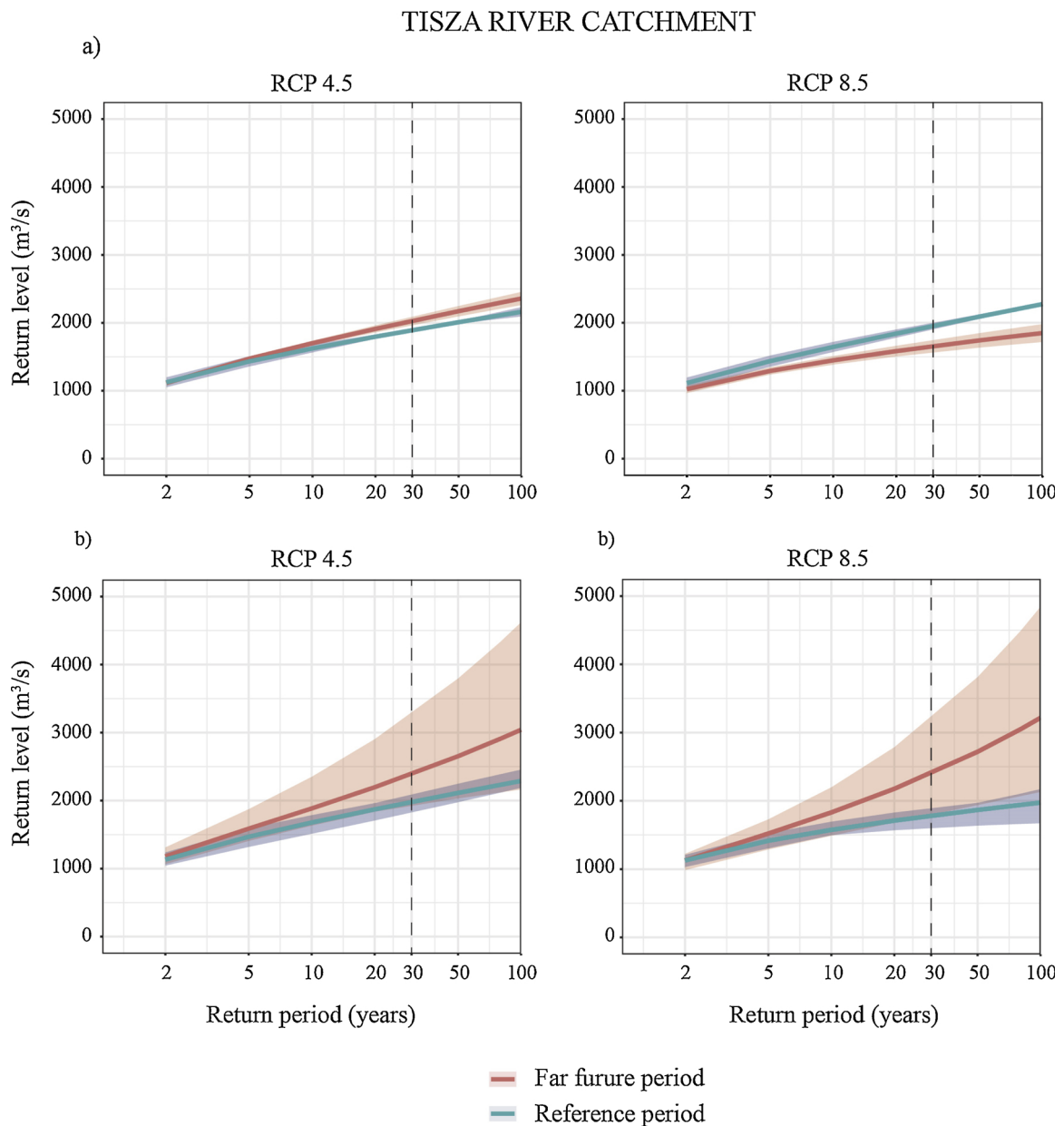


Fig. 5. Flood frequency curves of simulated discharge rates for a) GCM-XDS and b) GCM-RCM projections, based on the GEV distribution fit to the annual maxima in the reference and far future periods for the Tisza catchment.

2017). All these steps involve certain ranges of uncertainty in their outputs. Our study includes five different GCMs, two emission scenarios and different downscaling techniques: dynamical models and statistical-empirical approach, which were applied for two major Carpathian mountain river systems.

One of the issues affecting overall uncertainty can be related to the limited number of ensemble members. In our case, we used five GCMs (in total 11 scenarios – five under RCP 4.5 and six under RCP 8.5) to cover the range of temperature changes from 1 to 1.5 to more than 4° for the future period. In the paper of Dalelane et al. (2017) authors investigated approaches for decreasing the number of ensemble members. Their results show a decrease from 15 to 7 ensemble members, which still represent 90% of the original climate change signals (temperature and precipitation) in the future period compared to 1971-2000. We did not use method that has been mentioned above, but we can expect that the number of our ensemble members may be sufficient to include potential climate change signals.

Being an essential source area of freshwater for the Danube River, and due to its significance for tourism and recreation, the study region is very important for Ukraine, Romania and Moldova. Nevertheless, the region has been rarely investigated in the context of climate change until now.

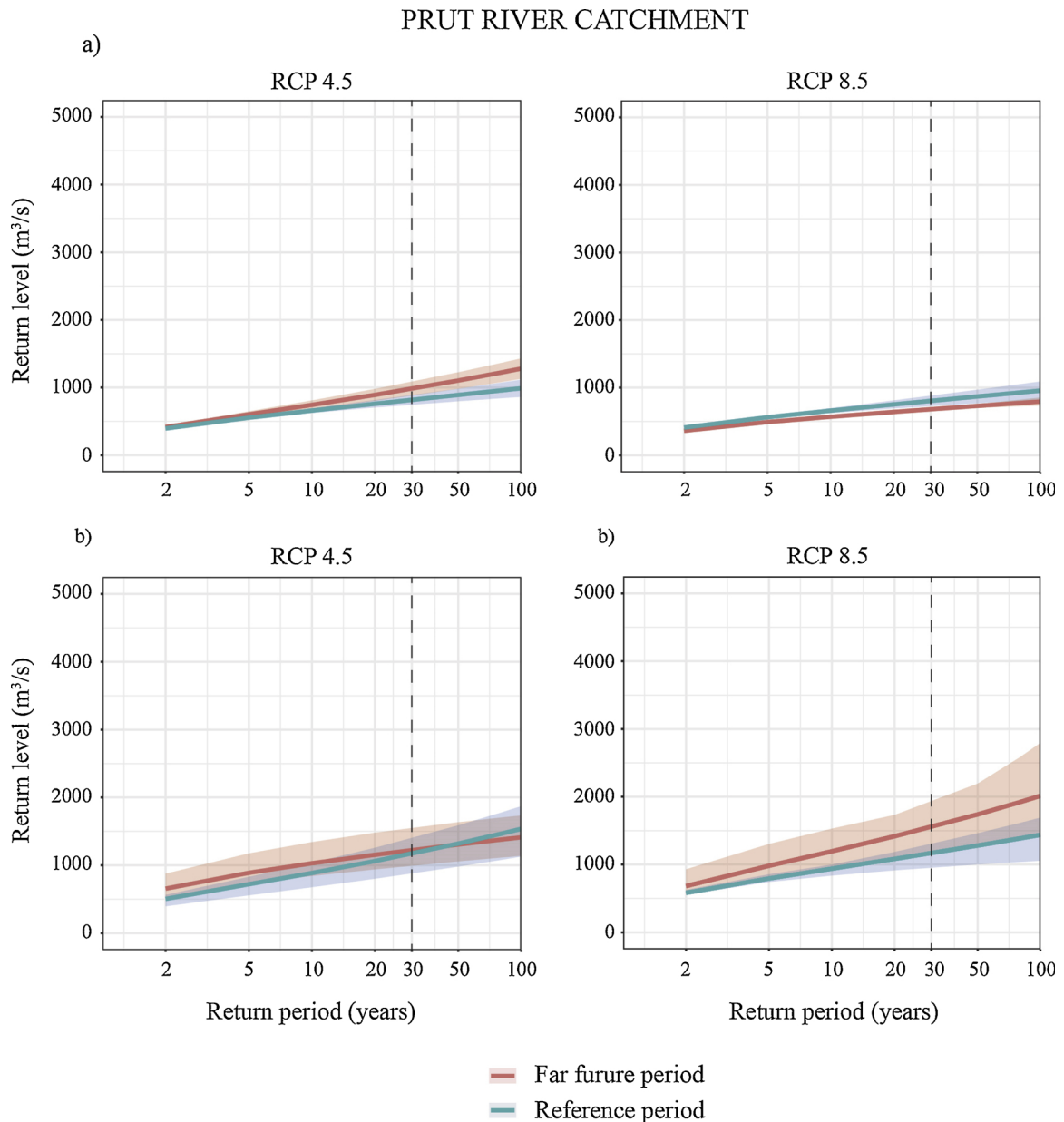


Fig. 6. Flood frequency curves of simulated discharge rates for a) GCMs-XDS and b) GCMs-RCM projections, based on the GEV distribution fit to the annual maxima in the reference and far future periods for the Prut catchment.

The quality of observational data plays a prominent role for the reliability of climate impact assessment. In the area under consideration, the number of climate stations is quite limited (12 stations in total, one station per 2500 km² on average), and the majority of stations are located in the lowland parts (only one station is located at an elevation above 900 m a.s.l.). The required interpolation of meteorological data to sub-basins in highlands can deteriorate the quality of input climate data for hydrological modelling. In addition, interpolation over relatively large distances may result in disregarding local extreme precipitation events. Uncertainty in precipitation, due to the lack of meteorological observation data in combination with specific climate conditions in the mountainous regions is a big issue. One of recommendations for reducing the uncertainty can be using additional climate data sources for improving calibration. Also, [Pluntke et al. \(2014\)](#) recommended to use alternative precipitation inputs and the ensemble approach to reduce the uncertainty. Nevertheless, the deviations of more than 2 °C in Tavr and 15% in precipitation for climate scenarios in the historical period after a bias correction are large. In case of RCM scenarios, one of possible source of uncertainty can appear from inconsistency between climate elements when doing an independent correction for each variable.

The relatively short duration of hydrological observations could increase uncertainty of estimation the return flood levels. Therefore, we did not explicitly analyse the 50 and 100 year floods but focused on the 30-year floods only. Uncertainty can also

originate from methods of river discharge measurements. In the case of extreme events, it is more difficult to estimate the specific peak rate correctly. For example, in our case data from the Tiszabecs and Vilok gauges, which are located close to each other, show inaccuracies, as during some high flow events the upstream gauge showed higher discharge values than the downstream one.

The impacts of water management in the catchments could also have significant effects on river runoff, particularly on droughts and to a lesser extent on extreme floods. In our study area there are no large reservoirs that could be modelled by SWIM, and the existing small ones are used for agriculture and fishing purposes. Most of them do not affect flood peaks notably. There are also dikes constructed as a part of flood protection measures. The abstracted water is distributed mainly among domestic uses and agriculture, and partly for industrial enterprises in both catchments under study. Unfortunately, missing information about water management during flooding periods did not allow us to take water management into account in this study. The uncertainty analysis related to climate projections showed that the scenarios have smaller biases for mean precipitation in the historical period, but the bias is much higher in the case of the 98 and 95 percentiles. This confirms that average conditions can be reflected much better by the combined climate and downscaling models than the extreme conditions (Bronstert et al., 2007).

As floods in the Tisza catchment occur in the fall-spring months, snow melt may play a prominent role in flooding processes. The bias in temperature in future climate projections can lead to uncertainties in the projected flood timing and magnitude, especially for the GCM-RCM driven scenarios, where bias in the historical period is up to 5 °C. Nevertheless, the type of the applied downscaling method is quite important, as the uncertainty due to such methods can be much higher compared to emission scenarios. In our study, there are inconsistent trends and different signals of change in projections obtained using RCMs and XDS, as well as among five GCMs.

6. Conclusions

In this work, we attempted to assess the potential climate change impacts on floods in the Carpathian region, considering the Upper Tisza and Upper Prut River catchments as case studies, which can be considered representative for western and eastern hydro-meteorological conditions in the high Carpathians.

The climate projections indicate an increase in the mean annual temperature under two RCPs in both catchments. The projected changes in precipitation show increases in the highland area in the majority of scenarios but for lowland the signal is not clear.

Based on the simulated time series for the future climate conditions, the analysis of changes in the magnitude of 30-year floods was done. The results show an increase of flood level for the majority of projections under RCP 4.5, ranging from 4.5 to 62% in the Tisza, and from 11 to 22% in the Prut. The moderate decreasing trends by 8–9% were detected just in one of five projections for each basin.

However, the projections under RCP 8.5 for both catchments are more uncertain: two of six projections indicate a decrease (up to 22%), three – an increase (up to 93–99%), and one shows negligible changes. The largest increases in the 30-year flood level exceeding 92% were simulated under IPSL-R-85 in both catchments, and exceeding 40% under Had-R for the Tisza (both RCPs) and Prut (RCP 8.5).

More significant changes in flood level were found for two projections driven by IPCL-R-85 and Had-R-85 in both catchments and for one projection driven by Had-R-45 in the Tisza catchment.

This study demonstrated the influence and sensitivity of different elements of the scenario and model chain on the projection of floods for the future. We want to emphasize that it is essential to include and analyse those uncertainties in the model-based impact assessment. In our case study, the choice of a particular GCM and downscaling technique has shown the strongest influence on the outputs. Due to the GCM-related uncertainty it was not possible to produce a clear and consistent picture of the future expected impacts on floods in the region. A bit surprising was that RCPs had a comparatively smaller influence, and were not consistent with the simulated changes, which were sometimes higher under RCP 4.5 than under RCP 8.5.

The annual mean change in precipitation was rather small, within $\pm 5\%$ in 64% of all projections (7 from 11) in both catchments, and it was ranging from +10 to +26% in four scenarios. Similar increasing trends for Eastern Europe were projected with different RCMs from the EURO-CORDEX (EEA, 2017)

Regarding simulation of the historical climate conditions, the GCM-XDS model combinations showed much lower bias in simulating temperature, and a bit lower in simulating precipitation compared to GCMs with the dynamical downscaling models. This can be explained by the method of downscaling and correction to data of climate stations. Regarding the future changes driven by GCMs downscaled by dynamical models and XDS, the impacts often show different patterns (see Figs. 5 and 6).

Furthermore, from our results we can conclude that the empirical/statistical downscaling method employed here produced smaller signals of change in flood levels and a smaller uncertainty compared to the dynamical downscaling method. This finding partly supports the conclusion of Bronstert et al. (2007) who found that methods like this, which were developed specifically to represent the climatological variance and/or anomalies, are particularly suitable for impact analysis of hydrological extremes. However, along with it the statistical methods can give an additional uncertainty in future projections in case of statistical relationship changes.

The emission and climate scenarios do not show a coherent and consistent picture regarding changes in precipitation in the case study region, leading to analogous uncertain results of impact assessment on river discharge and floods. In presented research the higher emission scenario (RCP 8.5) does not show a stronger trend in simulated river discharge than the moderate scenario (RCP 4.5).

In our opinion, the major reason for the generally large uncertainty of projections in this region is uncertainty stemming from the GCM simulations and low density of climate observations. Reducing uncertainties due to input data is a particular challenge for the Carpathian region, and it is essential for more reliable projections of floods in the future. So, it is important to improve the modelling

process by including additional data, more reliable climate scenarios and techniques.

Acknowledgements

Authors would like to thank the Global Runoff Data Centre for access to discharge data for the selected basins and the IMPRESSIONS project for the climate scenarios.

Appendix A. Supplementary data

Supplementary material related to this article can be found, in the online version, at doi:<https://doi.org/10.1016/j.ejrh.2019.01.002>.

References

- Aich, V., Liersch, S., Vetter, T., Huang, S., Tecklenburg, J., Hoffmann, P., Koch, H., Fournet, S., Krysanova, V., Müller, E.N., Hattermann, F.F., 2014. Comparing impacts of climate change on streamflow in four large African river basins. *Hydrol. Earth Syst. Sci. Discuss.* 18, 1305–1321. <https://doi.org/10.5194/hess-18-1305-2014>.
- Arnold, J.G., Allen, P.M., Bernhardt, G., 1993. A comprehensive surface-groundwater flow model. *J. Hydrol.* 142, 47–69. [https://doi.org/10.1016/0022-1694\(93\)90004-S](https://doi.org/10.1016/0022-1694(93)90004-S).
- Balabukh, V., Lukianets, O., 2015. Climate change and its consequences in Rakhiv district of Transcarpathian region. *Hydrol. Hydrochem. Hydroecology* 37, 132–148.
- Blöschl, G., Hall, J., Parajka, J., Perdigão, R.A.P., Merz, B., Arheimer, B., Aronica, G.T., Bilibashi, A., Bonacci, O., Borga, M., Čanjevac, I., Castellarin, A., Chirico, G.B., Claps, P., Fiala, K., Frolova, N., Gorbachova, L., Gül, A., Hannaford, J., Harrigan, S., Kireeva, M., Kiss, A., Kjeldsen, T.R., Kohnová, S., Koskela, J.J., Ledvinka, O., Macdonald, N., Mavrova-Guirguinova, M., Mediero, L., Merz, R., Molnar, P., Montanari, A., Murphy, C., Osuch, M., Ovcharuk, V., Radevski, I., Rogger, M., Salinas, J.L., Sauquet, E., Šraj, M., Szolgay, J., Viglione, A., Volpi, E., Wilson, D., Zaimi, K., Živković, N., 2017. Changing climate shifts timing of European floods. *Science* 357, 588–590. <https://doi.org/10.1126/science.aan2506>.
- Bronstert, A., Kolokotronis, V., Schwandt, D., Straub, H., 2007. Comparison and evaluation of regional climate scenarios for hydrological impact analysis: general scheme and application example. *Int. J. Climatol.* 27, 1579–1594. <https://doi.org/10.1002/joc.1621>.
- Bürger, G., 1996. Expanded downscaling for generating local weather scenarios. *Clim. Res.* 7, 111–128. <https://doi.org/10.3354/cr007111>.
- Bürger, G., Heistermann, M., Bronstert, A., 2014. Towards subdaily rainfall disaggregation via Clausius–Clapeyron. *J. Hydrometeorol.* 15, 1303–1311. <https://doi.org/10.1175/JHM-D-13-0161.1>.
- CGIAR-CSI. CGIAR-CSI SRTM 90m DEM Digital Elevation Database [WWW Document]. URL <http://srtm.csi.cgiar.org/> (Accessed 5 November 2017).
- Coles, S., 2001. An introduction to statistical modeling of extreme values. Springer Series in Statistics. Springer-Verlag, London, UK. <https://doi.org/10.1007/978-1-4471-3675-0>.
- Dalelane, C., Fruh, B., Steger, C., Walter, A., 2017. A pragmatic approach to build a reduced regional climate projection ensemble for Germany using the EURO-CORDEX 8.5 ensemble. *J. Appl. Met. Climatol.* 57 (3), 477–491. <https://doi.org/10.1175/JAMC-D-17-0141.1>. in press.
- Dankers, R., Christensen, O.B., Feyen, L., Kalas, M., de Roo, A., 2007. Evaluation of very high-resolution climate model data for simulating flood hazards in the Upper Danube Basin. *J. Hydrol.* 347, 319–331. <https://doi.org/10.1016/j.jhydrol.2007.09.055>.
- Didovets, I., Lobanova, A., Bronstert, A., Snizhko, S., Maule, C., Krysanova, V., 2017. Assessment of climate change impacts on water resources in three representative ukrainian catchments using eco-hydrological modelling. *Water* 9, 204. <https://doi.org/10.3390/w9030204>.
- Dobler, C., Bürger, G., Stötter, J., 2012. Assessment of climate change impacts on flood hazard potential in the Alpine Lech watershed. *J. Hydrol.* 460–461, 29–39. <https://doi.org/10.1016/j.jhydrol.2012.06.027>.
- Donat, M.G., Alexander, L.V., Yang, H., Durre, I., Vose, R., Caesar, J., 2013. Global land-based datasets for monitoring climatic extremes. *Bull. Am. Meteorol. Soc.* 94 (7), 997–1006. <https://doi.org/10.1175/BAMS-D-12-00109.1>.
- EEA, 2017. Climate Change, Impacts and Vulnerability in Europe: an Indicator-based Report, EEA Report. <https://doi.org/10.2800/66071>.
- FAO/IIASA/ISRIC/ISSCAS/JRC, 2012. Harmonized World Soil Database [WWW Document]. URL. (Accessed 15 November 2015). <http://webarchive.iiasa.ac.at/Research/LUC/External-World-soil-database/HTML/index.html?sb=1>.
- Gorbachova, L.O., Barandich, S.L., 2016. Spatio-temporal fluctuations of maximum flow of spring floods and snow-rain floods of Ukrainian rivers. *Sci. Proc. Ukr. Hydrometeorol. Ist.* 107–114.
- The Global Runoff Data Centre, 56068 Koblenz, Germany, 2017.
- Gupta, H.V., Sorooshian, S., Yapo, P.O., 1999. Status of automatic calibration for hydrologic models: comparison with multilevel expert calibration. *J. Hydrol. Eng.* 4, 135–143. [https://doi.org/10.1061/\(ASCE\)1084-0699\(1999\)4:2\(135\)](https://doi.org/10.1061/(ASCE)1084-0699(1999)4:2(135)).
- Hattermann, F.F., Post, J., Krysanova, V., Conrad, T., Wechsung, F., 2008. Assessment of water availability in a Central-European River Basin (Elbe) under climate change. *Adv. Clim. Change Res.* 4, 42–50.
- Huang, S., Hattermann, F.F., Krysanova, V., Bronstert, A., 2013. Projections of climate change impacts on river flood conditions in Germany by combining three different RCMs with a regional eco-hydrological model. *Clim. Change* 116, 631–663. <https://doi.org/10.1007/s10584-012-0586-2>.
- Huang, S., Kumar, R., Flörke, M., Yang, T., Hundecha, Y., Kraft, P., Gao, C., Gelfan, A., Liersch, S., Lobanova, A., Strauch, M., van Ogtrop, F., Reinhardt, J., Haberlandt, U., Krysanova, V., 2016. Evaluation of an ensemble of regional hydrological models in 12 large-scale river basins worldwide. *Clim. Change* 1–17. <https://doi.org/10.1007/s10584-016-1841-8>.
- International Commission for the Protection of the Danube River (ICPDR), 2009. Flood Action Programme Prut-Siret Sub-basin. Vienna. .
- IPCC, 2007. Climate change 2007 : impacts, adaptation and vulnerability : working Group II contribution to the Fourth Assessment Report of the IPCC Intergovernmental Panel on Climate Change. Work. Gr. II Contrib. to Intergov. Panel Clim. Chang. Fourth Assess. Rep. 1, 976. <https://doi.org/10.2134/jeq2008.0015br>.
- IPCC, 2014. Climate Change 2014: Mitigation of Climate Change: Contribution of Working Group III to the Fifth Assessment Report of the Intergovernmental Panel on Climate Change. Cambridge Univ. Press, pp. 1132.
- Jacob, D., Petersen, J., Eggert, B., Alias, A., Christensen, O.B., Bouwer, L.M., Braun, A., Colette, A., Déqué, M., Georgievski, G., Georgopoulou, E., Gobiet, A., Menut, L., Nikulin, G., Haensler, A., Hempelmann, N., Jones, C., Keuler, K., Kovats, S., Kröner, N., Kotlarski, S., Kriegsmann, A., Martin, E., van Meijgaard, E., Moseley, C., Pfeifer, S., Preuschmann, S., Radermacher, C., Radtke, K., Rechid, D., Rounsevell, M., Samuelsson, P., Somot, S., Soussana, J.F., Teichmann, C., Valentini, R., Vautard, R., Weber, B., Yiou, P., 2014. EURO-CORDEX: new high-resolution climate change projections for European impact research. *Reg. Environ. Change* 14, 563–578. <https://doi.org/10.1007/s10113-013-0499-2>.
- Kjellström, E., Nikulin, G., Hansson, U., Strandberg, G., Ullerstig, A., 2011. 21st century changes in the European climate: uncertainties derived from an ensemble of regional climate model simulations. *Tellus Ser. A Dyn. Meteorol. Oceanogr.* 63, 24–40. <https://doi.org/10.1111/j.1600-0870.2010.00475.x>.
- Koch, H., Liersch, S., Hattermann, F.F., 2013. Integrating water resources management in eco-hydrological modelling. *Water Sci. Technol.* 67, 1525–1533. <https://doi.org/10.2166/wst.2013.022>.
- Koch, H., Biewald, A., Liersch, S., de Azevedo, J.R.G., da Silva, G.N.S., Kölling, K., Fischer, P., Koch, R., Hattermann, F.F., 2015. Scenarios of climate and land-use change, water demand and water availability for the São Francisco River basin. *Rev. Bras. Ciências Ambient.* 96–114. <https://doi.org/10.5327/Z2176-947820151007>.
- Kohler, T., Giger, M., Hurni, H., Ott, C., Wiesmann, U., Wymann von Dach, S., Maselli, D., 2010. Mountains and climate change: a global concern. *Res. Dev.* 30, 53–55. <https://doi.org/10.1659/MRD-JOURNAL-D-09-00086.1>.

- Kok, K., Christensen, J.H., Madsen, M.S., Pedde, S., Gramberger, M., Jäger, J., Carter, T., 2015. Evaluation of Existing Climate and Socio-economic Scenarios Including a Detailed Description of the Final Selection [WWW Document]. URL. (accessed 2.17.17). http://impressions-project.eu/getatt.php?filename=attachme_12294.t.
- Köplin, N., Schädler, B., Viviroli, D., Weingartner, R., 2014. Seasonality and magnitude of floods in Switzerland under future climate change. *Hydrol. Process.* 28, 2567–2578. <https://doi.org/10.1002/hyp.9757>.
- Kormann, C., Francke, T., Renner, M., Bronstert, A., 2015. Attribution of high resolution streamflow trends in Western Austria - an approach based on climate and discharge station data. *Hydrol. Earth Syst. Sci. Discuss.* 19, 1225–1245. <https://doi.org/10.5194/hess-19-1225-2015>.
- Kovalets, I.V., Kivva, S., Udovenko, O.I., 2014. Usage of the WRF/DHSMV model chain for simulation of extreme floods in mountainous areas: a pilot study for the Uzh River Basin in the Ukrainian Carpathians. *Nat. Hazard.* <https://doi.org/10.1007/s11069-014-1412-0>.
- Kovats, R.S., Valentini, R., Bouwer, L.M., Georgopoulou, E., Jacob, D., Martin, E., Rounsevell, M., Soussana, J., 2014. *Climate Change 2014: Impacts, Adaptation, and Vulnerability. Part B: Regional Aspects. Contribution of Working Group II to the Fifth Assessment Report of the Intergovernmental Panel on Climate Change.* Cambridge University Press, Cambridge and New York.
- Krakovska, S., Balabukh, V., Palamarchuk, L., Djukel, G., Gnatiuk, N., 2012. Analysis and projections of climate change impacts on flood risks in the Dniester river basin based on the ENSEMBLES RCM data. *Geophysical Research Abstracts*, Vienna.
- Krysanova, V., Meiner, A., Roosaare, J., Vasilyev, A., 1989. Simulation modelling of the coastal waters pollution from agricultural watershed. *Ecol. Model.* 7–29.
- Krysanova, V., Wortmann, M., Bolch, T., Merz, B., Duethmann, D., Walter, J., Huang, S., Tong, J., Buda, S., Kundzewicz, Z.W., 2015. Analysis of current trends in climate parameters, river discharge and glaciers in the Aksu River basin (Central Asia). *Hydrol. Sci. J. Des Sci. Hydrol.* 60, 566–590. <https://doi.org/10.1080/02626667.2014.925559>.
- Kynal, O., Kholiavchuk, D., 2016. Climate variability in the mountain river valleys of the Ukrainian Carpathians. *Quat. Int.* 415, 154–163. <https://doi.org/10.1016/j.quaint.2015.12.053>.
- Lobanova, A., Liersch, S., Tàbara, J.D., Koch, H., Hattermann, F.F., Krysanova, V., 2017. Harmonizing human-hydrological system under climate change: a scenario-based approach for the case of the headwaters of the Tagus River. *J. Hydrol.* 548, 436–447. <https://doi.org/10.1016/j.jhydrol.2017.03.015>.
- Meresa, H.K., Romanowicz, R.J., Napiorkowski, J.J., 2017. Understanding changes and trends in projected hydroclimatic indices in selected Norwegian and Polish catchments. *Acta Geod. Geophys. Hung.* 65, 829–848. <https://doi.org/10.1007/s11600-017-0062-5>.
- Mitchell, T.D., Carter, T.R., Jones, P.D., Hulme, M., New, M., 2004. A comprehensive set of high-resolution grids of monthly climate for Europe and the globe: the observed record (1901–2000) and 16 scenarios (2001–2100). *Cent. Clim.* 1–30. <https://doi.org/10.1016/j.biocon.2014.11.027>.
- Moriasi, D.N., Arnold, J.G., Van Liew, M.W., Binger, R.L., Harmel, R.D., Veith, T.L., 2007. Model evaluation guidelines for systematic quantification of accuracy in watershed simulations. *Trans. ASABE* 50, 885–900. <https://doi.org/10.13031/2013.23153>.
- Mueller, E.N., Pfister, A., 2011. Increasing occurrence of high-intensity rainstorm events relevant for the generation of soil erosion in a temperate lowland region in Central Europe. *J. Hydrol.* 411, 266–278. <https://doi.org/10.1016/j.jhydrol.2011.10.005>.
- Nash, J.E., Sutcliffe, J.V., 1970. River flow forecasting through conceptual models part I—a discussion of principles. *J. Hydrol.* 10, 282–290. [https://doi.org/10.1016/0022-1694\(70\)90255-6](https://doi.org/10.1016/0022-1694(70)90255-6).
- Open Street Map contributors, 2017. OpenStreetMap Data [WWW Document]. URL. (Accessed 08 October 2017). <https://www.openstreetmap.org/#map=5/47.739/16.040>.
- Patterson, T., Kelso, N., 2016. Natural Earth [WWW Document]. URL. (Accessed 7 November 2016). <http://www.naturalearthdata.com/>.
- Petrow, T., Zimmer, J., Merz, B., 2009. Changes in the flood hazard in Germany through changing frequency and persistence of circulation patterns. *Nat. Hazards Earth Syst. Sci. Discuss.* 9, 1409–1423. <https://doi.org/10.5194/nhess-9-1409-2009>.
- Piniewski, M., Szczeniński, M., Kundzewicz, Z.W., Mezghani, A., Hov, Ø., 2017. Changes in low and high flows in the Vistula and the Odra basins: model projections in the European-scale context. *Hydrol. Process.* 31, 2210–2225. <https://doi.org/10.1002/hyp.11176>.
- Pluntke, T., Pavlik, D., Bernhofer, C., 2014. Reducing uncertainty in hydrological modelling in a data sparse region. *Environ. Earth Sci.* 72, 4801. <https://doi.org/10.1007/s12665-014-3252-3>.
- Quintana-Seguí, P., Habets, F., Martin, E., 2011. Comparison of past and future Mediterranean high and low extremes of precipitation and river flow projected using different statistical downscaling methods. *Nat. Hazards Earth Syst. Sci. Discuss.* 11, 1411–1432. <https://doi.org/10.5194/nhess-11-1411-2011>.
- Renard, B., Lang, M., Bois, P., Dupeyrat, A., Mestre, O., Niel, H., Sauquet, E., Prudhomme, C., Parys, S., Paquet, E., Neppel, L., Gailhard, J., 2008. Regional methods for trend detection: assessing field significance and regional consistency. *Water Resour. Res.* 44. <https://doi.org/10.1029/2007WR006268>.
- Roudier, P., Andersson, J.C.M., Donnelly, C., Feyen, L., Greuell, W., Ludwig, F., 2016. Projections of future floods and hydrological droughts in Europe under a +2°C global warming. *Clim. Change* 135, 341–355. <https://doi.org/10.1007/s10584-015-1570-4>.
- Seneviratne, S.I., Donat, M.G., Mueller, B., Alexander, L.V., 2014. No pause in the increase of hot temperature extremes. *Nat. Clim. Change* 4 (3), 161–163. <https://doi.org/10.1038/nclimate2145>.
- Spinoni, J., Szalai, S., Szentimrey, T., Lakatos, M., Bihari, Z., Nagy, A., Németh, Á., Kovács, T., Mihic, D., Dacic, M., Petrovic, P., Kržič, A., Hiebl, J., Auer, I., Milkovic, J., Štepanek, P., Zahradnick, P., Kilar, P., Limanowka, D., Pyrc, R., Cheval, S., Birsan, M.V., Dumitrescu, A., Deak, G., Matei, M., Antolovic, I., Nejedlik, P., Štastný, P., Kajaba, P., Bochnicek, O., Galo, D., Mikulová, K., Nabyvanets, Y., Skrynyk, O., Krakovska, S., Gnatiuk, N., Tolasz, R., Antofie, T., Vogt, J., 2015. Climate of the Carpathian Region in the period 1961–2010: climatologies and trends of 10 variables. *Int. J. Climatol.* 35, 1322–1341. <https://doi.org/10.1002/joc.4059>.
- Stahl, K., Hisdal, H., Hannaford, J., Tallaksen, L.M., Van Lanen, H.A.J., Sauquet, E., Demuth, S., Fendekova, M., Jodar, J., 2010. Streamflow trends in Europe: evidence from a dataset of near-natural catchments. *Hydrol. Earth Syst. Sci. Discuss.* 14, 2367–2382. <https://doi.org/10.5194/hess-14-2367-2010>.
- Themeßl, M.J., Gobiet, A., Heinrich, G., 2012. Empirical-statistical downscaling and error correction of regional climate models and its impact on the climate change signal. *Clim. Change* 112, 449–468. <https://doi.org/10.1007/s10584-011-0224-4>.
- U.S. Dept. of the Interior, U.S.G.S., 2005. Global Visualization Viewer [WWW Document]. URL. (Accessed 8 October 2015). <http://glovis.usgs.gov/>.
- U.S. Geological Survey, 2016. Landsat 5 History [WWW Document]. URL. (Accessed 7 November 2015). <https://landsat.usgs.gov>.
- Veijalainen, N., Lotsari, E., Alho, P., Vehviläinen, B., Käyhkö, J., 2010. National scale assessment of climate change impacts on flooding in Finland. *J. Hydrol.* 391, 333–350. <https://doi.org/10.1016/j.jhydrol.2010.07.035>.
- Villarini, G., Smith, J.A., Serinaldi, F., Ntelekos, A.A., 2011. Analyses of seasonal and annual maximum daily discharge records for central Europe. *J. Hydrol.* 399, 299–312. <https://doi.org/10.1016/j.jhydrol.2011.01.007>.
- Vormoor, K., Lawrence, D., Heistermann, M., Bronstert, A., 2015. Climate change impacts on the seasonality and generation processes of floods - projections and uncertainties for catchments with mixed snowmelt/rainfall regimes. *Hydrol. Earth Syst. Sci. Discuss.* 19, 913–931. <https://doi.org/10.5194/hess-19-913-2015>.
- Weedon, G.P., Balsamo, G., Bellouin, N., Gomes, S., Best, M.J., Viterbo, P., 2014. Data methodology applied to ERA-Interim reanalysis data. *Water Resour. Res.* 50, 7505–7514. <https://doi.org/10.1002/2014WR015638>. Received.
- Wilson, D., Hisdal, H., Lawrence, D., 2010. Has streamflow changed in the Nordic countries? - Recent trends and comparisons to hydrological projections. *J. Hydrol.* 394, 334–346. <https://doi.org/10.1016/j.jhydrol.2010.09.010>.
- World Health Organization, 2017. Floods in Moldova, Romania and Ukraine (summer 2008) [WWW Document]. URL. (Accessed 28 November 2017). <http://www.euro.who.int/en/health-topics/emergencies/disaster-preparedness-and-response/policy/response/floods-2008>.
- Wortmann, M., Bolch, T., Krysanova, V., Buda, S., 2016. Bridging glacier and river catchment scales: an efficient representation of glacier dynamics in a hydrological model. *Hydrol. Earth Syst. Sci. Discuss.* 1–37. <https://doi.org/10.5194/hess-2016-272>.
- Wosten, J., Pachepsky, Y.A., Rawls, W.J., 2001. Pedotransfer functions: Bridging the gap between available basic soil data and missing soil hydraulic characteristics. *J. Hydrol.* 251, 123–150. [https://doi.org/10.1016/S0022-1694\(01\)00464-4](https://doi.org/10.1016/S0022-1694(01)00464-4).